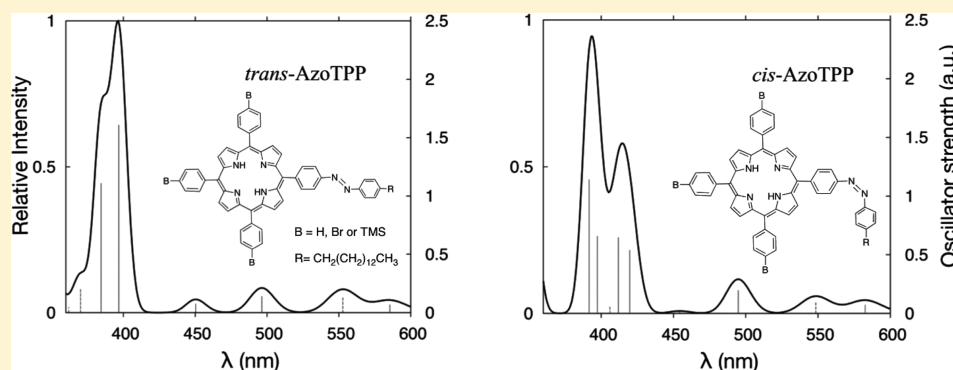# Theoretical Study of Novel Azo-Tetraphenylporphyrins: Potential Photovoltaic Materials

Elizabeth Hernandez-Marin,[†] Carolina Caicedo,[†] Ernesto Rivera, and Ana Martínez*

Instituto de Investigaciones en Materiales, Universidad Nacional Autónoma de México, Circuito Exterior SN. Ciudad Universitaria, C.P. 04510 Coyoacán, Mexico City, Mexico

S *Supporting Information*

ABSTRACT: A density functional theory study was performed to analyze the electron donor–acceptor properties of the cis and trans isomers of a novel azobenzene-containing tetraphenylporphyrin ($TPPN_2PhC_{14}H_{29}$) with different substituents (Br or TMS). In general, the trans isomers are better electron acceptors than the correspondent cis homologues. Their UV–vis spectra were also obtained and a comparison with available experimental results is included. According to these results, the azo compounds reported here are promising materials for the elaboration of dye-sensitized solar cells because their HOMO–LUMO gaps are close to 2 eV. Moreover, the energy of the high intensity absorption bands also fulfills the requirements needed for the operation of a solar cell built with TiO_2 and the I^-/I_3^- pair.

INTRODUCTION

Porphyrins are a very important family of fluorophores that have been widely used in macromolecular and materials science.[1−4] These conjugated compounds are highly delocalized π-systems that are considered as outstanding ionic scavengers, whose recognition properties arise from the heteroatoms present in their structure.[5] Porphyrins have been the subject of intense research for the development of solar energy transfer and electron transfer systems, due to their efficient light absorption.[6−10] Free-base porphyrins usually exhibit an intense Soret band at ca. λ = 420 nm in their absorption spectra, followed by four weak Q bands which appear between λ = 500 and 700 nm and are visible for all compounds. These chromophores have been incorporated into polymers, allowing the easy handling, recycling, and adapting of these complexing agents to different processes.[11,12] These molecules have also been employed in the design of push–pull π conjugated systems bearing donor–acceptor groups and in the design of dendritic molecules able to act as molecular antennae for photovoltaic applications.[6−8] The design of new porphyrins and multiporphyrinic arrays is very attractive due to its application in nonlinear optics (NLO),[2] two-photon absorption,[3] and molecular wires.[4] Several electro- and photoactive units have been incorporated into porphyrins to tune their electronic and photophysical properties. The donor–acceptor character of porphyrins can also be modified depending on their coordination state and the photoactive units linked to the molecules.[13−18] Thus, the preparation and properties of various porphyrin derivatives linked to electro- and photoactive units such as fullerene C_{60},[13] anthracene,[14,15] pyrene,[16−18] and functionalized porphyrins,[19] have been published in the literature. In particular, our research focuses on the design of molecular antennae and push–pull π-conjugated systems, so that we have synthesized and characterized some soluble precursor porphyrin derivatives able to act as either donor or acceptor groups.[20,21]

Rau[22] classified azobenzenes into three main groups on the basis of their photochemical behavior.[23] Unsubstituted photochromic azobenzene makes up the first group, known as "azobenzenes". The thermally stable trans isomer exhibits a strong π–π* transition at 350 nm and a weak n–π* transition at 440 nm, whereas the cis isomer undergoes similar transitions but with a more intense n–π* band. In addition, "azobenzenes" have a relatively poor π–π* and n–π* overlap. The second

B = H, Br or TMS

R= $CH_2(CH_2)_{12}CH_3$

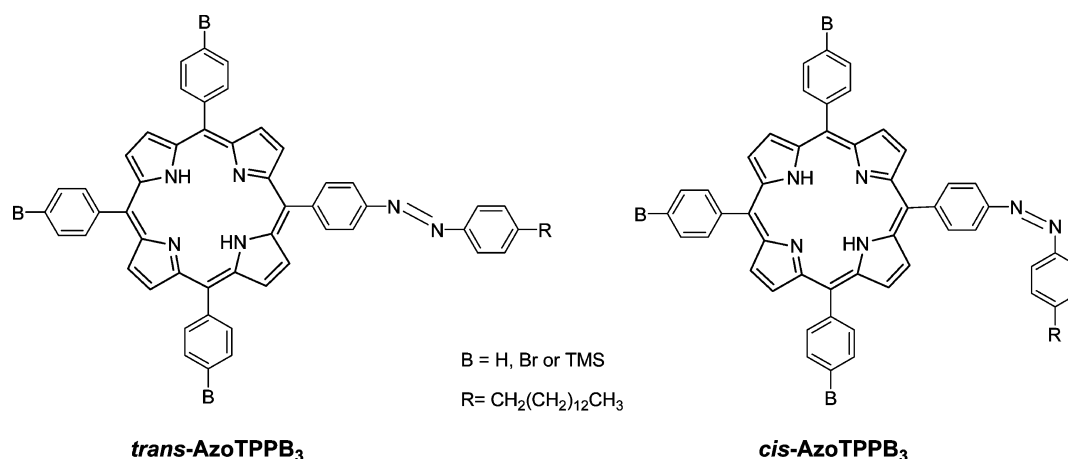*trans*-AzoTPPB₃

cis-AzoTPPB₃

Figure 1. Schematic representation of the azo compounds under study.

group, known as "aminoazobenzenes" typically includes azobenzenes that are substituted by an electron-donor group and are characterized by the overlapping of the $\pi-\pi^*$ and $n-\pi^*$ bands. Finally, azobenzenes bearing both electron-donor and electron-acceptor groups belong to the third category, "pseudostilbenes", where the $\pi-\pi^*$ and $n-\pi^*$ bands are practically superimposed and inverted on the energy scale with respect to the "azobenzene" bands. When donor–acceptor substituted azobenzenes are incorporated into a polymer backbone or side chain, they provide very versatile materials from the applications point of view. In particular, "pseudostilbene" azobenzenes undergo rapid trans–cis–trans photo-isomerization when they are irradiated with linear polarized light. The use of polarized light allows the selective activation of "pseudostilbenes" with the polarization axis parallel to the absorbing radiation.[23] Therefore, azobenzene containing polymers and azo-dyes have been considered as versatile materials due to the photoinduced motions which occur on them after irradiation with linear polarized light.[23] Particularly, the π-conjugated porphyrin–azobenzene systems showed to be efficient light-responsive materials with potential applications in optical storage.[24−29] Our research group has previously reported the synthesis and characterization of a large series of azobenzene based materials (azo-dyes,[30−33] azo-polymers,[34−38] and azo-dendrons[39,40]). Additionally, porphyrin–azobenzene molecules have attracted the interest of the scientific community because their optical properties can be modified photochemically.[41−43] The extension of the conjugation length in porphyrin systems can be augmented by coupling them with other aromatic units via molecular bridges consisting of alkenes, alkynes, imines, and other unsaturated functional groups,[44−49] the azo group (N═N) being the best option for this purpose, as has been demonstrated by Anderson and co-workers.[3,4] The azoporphyrins exhibit a strong interaction between the phenyl rings and the azo bridge.[49] These molecules are promising candidates for photonic applications because they also exhibit nonlinear optical properties (NLO) of third harmonic generation (THG).

The interest for photochromic molecules is also due to the electronic and geometrical changes that can take place on them, for example, the reversible photomodulation (photoswitching) that allows the trans–cis isomerization of azobenzenes. Although porphyrins are moderate emitters, the quantum yield of the trans–cis photoisomerization of a low dipole moment azobenzene–porphyrin system is very high and can be

monitored by UV−vis spectroscopy. After irradiation, the $\pi-\pi^*$ band, which is more intense for the trans isomer, decreases in intensity whereas the $n-\pi^*$ band becomes more intense. However, this reaction is reversible and the cis isomer goes back to the trans form.[23] In this context, the synthesis of an azo-porphyrin (TPPN₂PhC₁₄H₂₉) has been reported and the influence of the porphyrin ring and trans−cis photoisomeriza-tion on the optical properties was analyzed.[21] In a previous work, we reported a theoretical study of a series of substituted porphyrins bearing donor and acceptor groups.[50] Herein, we report a theoretical study of the trans and cis isomers of three azobenzene−porphyrin systems AzoTPPB₃ (Figure 1), where B = H, Br, and Si(CH₃)₃ (TMS), to predict their main absorption bands, and the nature of the electronic excitations. Moreover, their electron donor−acceptor characteristics have been studied in detail to provide information for the future design and synthesis of promising photoresponsive and photovoltaic materials. The advantage of working with a low dipole moment azobenzene system containing porphyrin units is that it behaves as an "azobenzene" according to the Rau classification, so it is necessary to irradiate with UV light to promote the trans−cis isomerization. In consequence, the trans−cis isomerization of azo-porphyrin (TPPN₂PhC₁₄H₂₉) can be promoted by irradiating with light exciting the molecule at λ = 400 nm (wavelength of the $\pi-\pi^*$, near the Soret band). Therefore, these azobenzene−porphyrin systems can give the first photoinduced motion of azobenzenes (trans−cis isomer-ization) after irradiation. Also, the interaction of porphyrins with other chromophores can give FRET (fluorescence resonance energy transfer) phenomena.[8] In this case porphyr-ins can act as either donor or acceptor groups depending on the nature of the partner chromophore. Because (TPPN₂PhC₁₄H₂₉) shows a wide absorption in the UV−vis range (from 370 to 668 nm) this dye can be used in absorption dye-sensitized solar cells (DSSC).

■ COMPUTATIONAL DETAILS AND THEORETICAL METHODS

The density functional theory (DFT) approximation[51,52] as implemented in Gaussian 09[53] was used for all calculations that were carried out using the B3LYP functional[54−56] and the 6-31g(d,p) basis set.[57,58] Full geometry optimization without symmetry constraints were carried out for all the stationary points. Harmonic frequency analysis allowed us to verify the optimized minima. The local minima were identified when the
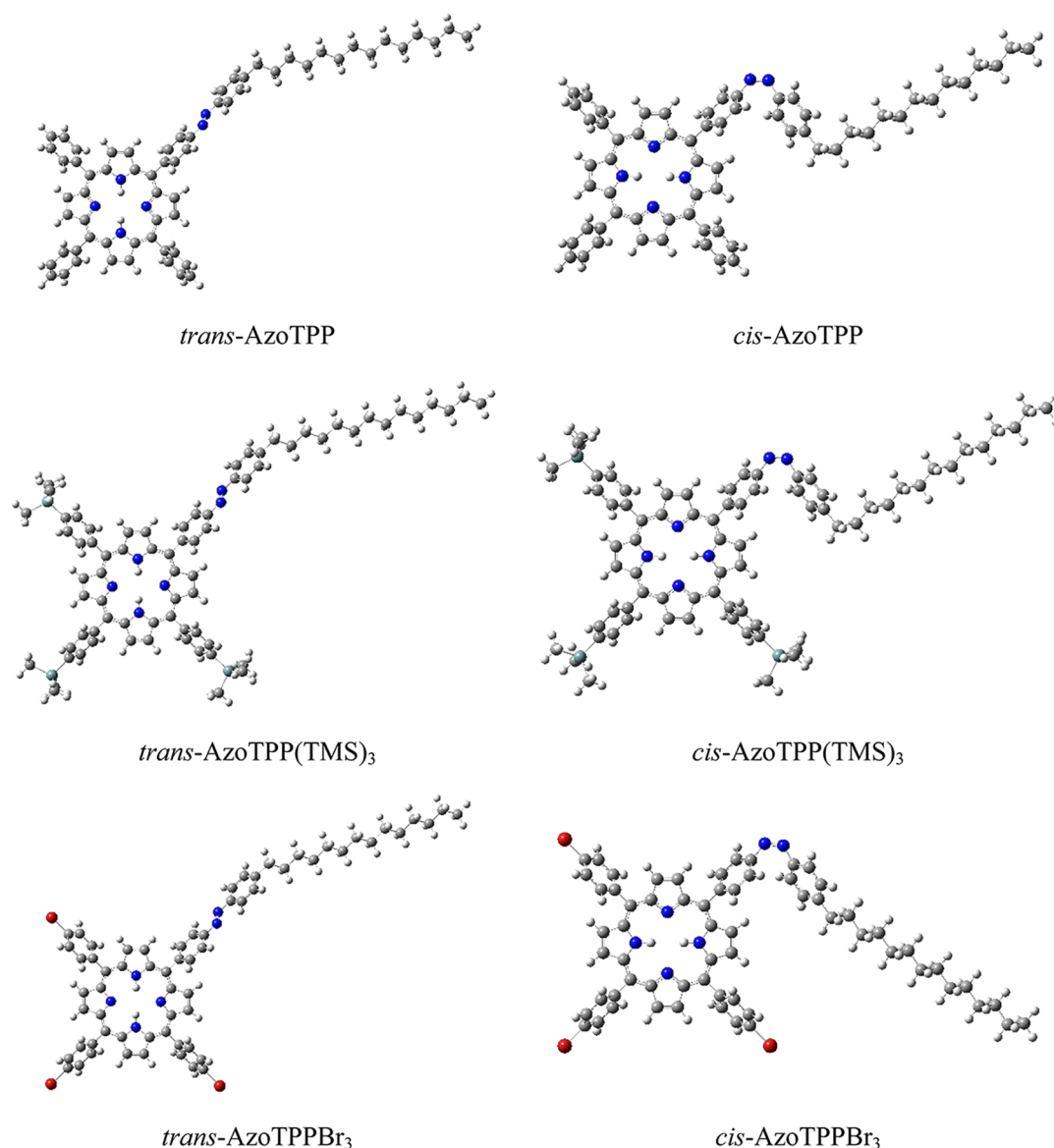
198

dx.doi.org/10.1021/jp408194c | J. Phys. Chem. A 2014, 118, 197−207

trans-AzoTPP

cis-AzoTPP

trans-AzoTPP(TMS)$_3$

cis-AzoTPP(TMS)$_3$

trans-AzoTPPBr$_3$

cis-AzoTPPBr$_3$

Figure 2. Optimized structures of the six isomers under study.

number of imaginary frequencies is equal to zero. The absorption spectra have been computed with time-dependent density functional theory (TD-DFT) using B3LYP functional and the same basis sets. Theoretically, the intensity of the band is expressed in terms of the oscillator strengths (f). Stationary points were first modeled in the gas phase (vacuum), and solvent effects were included a posteriori, applying single point calculations at the same level of theory, using a polarizable continuum model, specifically the integral-equation-formalism (IEF-PCM)[59,60] with chloroform as solvent to make a comparison with available experimental results. Previous TD-DFT benchmark reports[61] indicate that the results obtained with B3LYP are in good agreement with experimental values. The mean absolute error that they reported is in the range of 5.8 and 21 nm. The analysis of the changes in electron density for a given electronic transition was based on the electron density difference maps (EDDMs) constructed using the GaussSum suite of programs.[62]

Gázquez and co-workers[63,64] have proposed two different electronegativities (χ) for the charge transfer process: one that describes fractional negative charge donation (χ^-) whereas the other gives the fractional negative charge acceptance (χ^+):

$$\chi^- = 0.25(3I + A) \tag{1}$$

$$\chi^+ = 0.25(I + 3A) \tag{2}$$

where I (vertical ionization energy) and A (vertical electron affinity) refer to one-electron transfer processes. Because the partial charge transfer is one of the main intermolecular factors that dominates the binding energies in many reactions, χ^- and χ^+ should be better parameters than I and A to describe the electron donor–acceptor properties of these systems. Thus, the construction of a so-called donor–acceptor map (DAM) has been suggested.[65] A DAM can be constructed by plotting the values of χ^- (y-axis) and χ^+ (x-axis) for each molecule of interest. Low values of both χ^- and χ^+ represent a good electron donor molecule, whereas high values imply a good electron-acceptor species. This would imply that electrons could be transferred from a good donor to an acceptor, which is expected to be located up (high value of χ^-) and to the right (high value of χ^+) of the donor. Therefore, the DAM is a very

199

dx.doi.org/10.1021/jp408194c | J. Phys. Chem. A 2014, 118, 197−207

useful tool for qualitative comparison because any compound can be classified in terms of its electron-donating−accepting capabilities.

RESULTS AND DISCUSSION

The optimized structures of the six azo-porphyrins (three trans and three cis isomers) under study are reported in Figure 2.

The average dihedral angle between the porphyrin ring and the phenyl rings varies between 64.03° (*trans*-AzoTPPBr$_3$) and 64.87° (*cis*-AzoTPP(TMS)$_3$); see Table S1 in the Supporting Information. The C—N=N—C dihedral angle is very close to 180° for the three trans isomers and 10.0°, 10.5°, and 10.6° for *cis*-AzoTPP(TMS)$_3$, *cis*-AzoTPPBr$_3$, and *cis*-AzoTPP, respectively. The C−H, C−Br, and C−Si bond lengths (1.09, 1.91, and 1.90 Å, respectively) are within the expected values (1.12, 1.94, and 1.87 Å) for such bonds.[66] The N=N bond length is equal to 1.26 Å for all trans isomers and 1.25 Å for all cis isomers (Table S1 of the Supporting Information). The C—N bond lengths are 1.42 Å for all trans isomers and 1.43 Å for all cis isomers. The trans isomers are more stable than the cis isomers by 16 kcal/mol approximately (Table S1 of the Supporting Information), in the three systems. If we compare these relative energies with the calculated energy difference between *cis*- and *trans*-azobenzene (15 kcal/mol, Table S1, Supporting Information), the values are very similar and it is possible to say that the addition of the porphyrin group does not affect the relative energies of the cis and trans isomers of the azobenzene. To roughly estimate the activation energy for the trans−cis isomerization process, structures of the AzoTPP compounds and of azobenzene (AB), 4-aminoazobenzene (AAB), 4-nitroazobenzene (NAB), and 4-methoxyazobenzene (MAB) with a C−N−N−C dihedral angle frozen to 90° were optimized. These structures will be referred to as "pseudo-transition state structures" (pTS). Additionally, the trans and cis structures of azobenzene, AAB, NAB, and MAB were fully optimized. The trend followed by the values of the energy differences between the energy of the pTS structures and their respective AB, AAB, and NAB trans isomers indicate that −NO$_2$ (an electron withdrawing group) decreases more the activation energy, with respect to azobenzene, than the electron donor −NH$_2$ (Table S2, Supporting Information). This trend matches well with the results reported by Wazzan et al.[67] who studied the cis to trans process. It can also be seen in Table S2 (Supporting Information) that −NO$_2$ stabilizes the cis isomer more, with respect to azobenzene, than −NH$_2$. The results for MeO suggest that this electron-donating group decreases the trans to cis activation energy less than −NH$_2$ but destabilizes the cis isomer in the same way as −NH$_2$. Now, with respect to AzoTPP, AzoTPP(TMS)$_3$, and AzoTPPBr$_3$, the calculated energy differences between the pTS and its respective trans species are around 2.36 eV (Table S2, Supporting Information). These values are slightly smaller than the energy difference calculated for azobenzene (2.39 eV, Table S2, Supporting Information). This could suggest that in the AzoTPP compounds both the porphyrin ring and the aliphatic chain behave more like electron donating groups due to inductive effects. Thus, it could be expected that the experimental activation energy for the thermal isomerization of the AzoTPP compounds under study would fall in the interval 0.8−1 eV, where the first value corresponds to the experimental activation energy determined for the cis to trans isomerization of AAB,[67] and the latter value corresponds to the activation energy determined for azobenzene.[68]

The electron donor−acceptor properties of the azo-porphyrins are very helpful to determine their electron transfer capabilities. This is significant if we consider their potential use in dye-sensitized solar cells (DSSC). Because in the archetypical DSSC the dye is attached to the surface of a layer composed of a network of TiO$_2$ particles,[69] it is important to establish the relative electron transfer capabilities of the dye (in this case, the azo-porphyrin) and TiO$_2$. As the DSSC is exposed to the environment, it is necessary to predict if the dye would be prone to attack by some reactive oxygen species, such as the following free radicals: $^\bullet$O$_2^-$, $^\bullet$OH, or $^\bullet$OOH. Figure 3
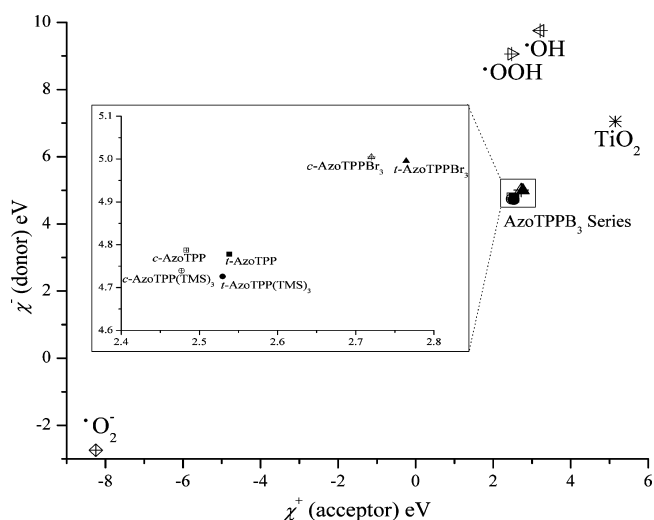

Figure 3. DAM for the cis and trans isomers of the azo compounds under study, some reactive oxygen species ($^\bullet$O$_2^-$, $^\bullet$OH, and $^\bullet$OOH), and TiO$_2$.

shows the DAM for the six azo compounds under study, $^\bullet$O$_2^-$, $^\bullet$OH, and $^\bullet$OOH. TiO$_2$ is included in Figure 3, considering a value for the vertical ionization energy ≈8 eV (Chiodo et al.[70]) and that the vertical electron affinity is ≈4.2 eV (Fuke et al.[71]).

It was already mentioned that the DAM is a very useful qualitative tool to quickly assess the donor−acceptor character of a series of molecules placed within the map. In Figure 3, it can be seen that $^\bullet$O$_2^-$ is a good electron-donor (low values of both χ^- and χ^+). It was also mentioned previously that the negative charge will transfer from one molecule (thus considered the donor) to another one located to the right of the first molecule. In Figure 3, the azo compounds, TiO$_2$ and the other two free radicals are located markedly up to the right of $^\bullet$O$_2^-$. This fact, in principle, may indicate that $^\bullet$O$_2^-$ should be able to transfer an electron to any of the other species.

Now, considering the other free radicals ($^\bullet$OH and $^\bullet$OOH), they are only slightly up to the right of the azo compounds and TiO$_2$. Therefore, the electron transfer reaction between the free radicals and the azo compounds or TiO$_2$ is not necessarily expected because their values of electronegativity are similar.

The presence of Br increases noticeably the values of χ^- and χ^+ with respect to the other azo compounds. This means that the AzoTPPBr$_3$ isomers are worse electron donors and better electron acceptors than AzoTPP and AzoTPP(TMS)$_3$. In all cases, the trans isomers are slightly better electron acceptors (i.e., its χ^- is larger) than their corresponding cis homologues. This could be due to the nature of the lowest unoccupied molecular orbital (LUMO). For the trans species, the LUMO includes π interactions that are localized on the porphyrin

system and the azo group, allowing a more stable distribution of the charge, whereas the LUMO of the cis isomers is a π distribution localized mainly in the porphyrin unit. Finally, on the basis of their values of χ^+, TiO$_2$ appears to be (as desired) a better electron acceptor than any of the azo compounds considered here because its χ^+ value is larger. Likewise, on the basis of the values of χ^-, TiO$_2$ appears to be a worst electron donor than any of the azo compounds because its χ^- is larger. Therefore, on the basis of their donor−acceptor properties, the AzoTPP compounds presented here are promising materials for further development of novel DSSCs.

Given that useful materials for the design of photovoltaic cells must absorb most of the radiation from the solar light in the near-IR and visible regions, the energy difference between the highest occupied molecular orbital (HOMO) and lowest unoccupied molecular orbital (LUMO) of the light-absorbing material is crucial. Thus, if the maximum in the solar radiation energy spectrum corresponds to 2 eV, it is desirable that the HOMO−LUMO energy gap approximates this value. Moreover, if the materials used in the construction of the cell are for example TiO$_2$ and the pair I$^-$/I$_3^-$ as the electrolyte, it is also desirable that the LUMO of the dye lies above the conduction band (CB) of TiO$_2$ (−4.2 eV), whereas the HOMO should be below the I$^-$/I$_3^-$ redox potential (around −4.90 eV).[72] To establish the possible use of these azo compounds as possible DSSC materials, it is important to take into account their HOMO−LUMO gap and their respective HOMO and LUMO energies. The molecular energy diagram is presented in Figure 4. For comparison, the ZnTPP-C porphyrin[71] (C contains a
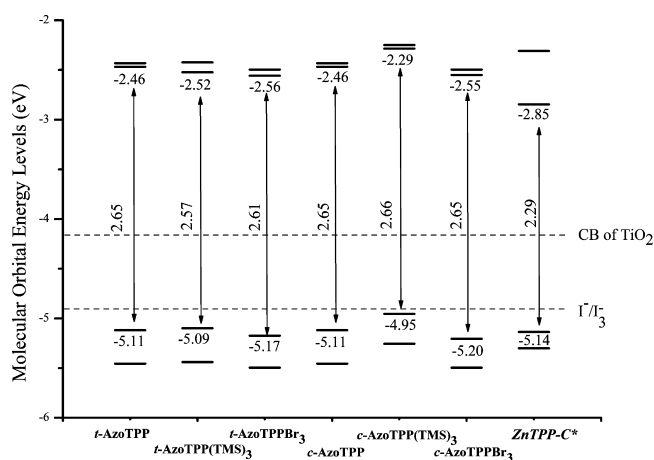

Figure 4. Molecular orbital energy diagram for the *cis*- and *trans*-AzoTPPB$_3$ compounds. ZnTPP-C was reported in ref 20. CB is the conduction band of titanium oxide and I$^-$/I$_3^-$ represents the electrolyte.

thiophene group between a methyne and cyanoacrylic acid groups) reported before and calculated as well within the B3LYP approximation, is also included.

In all cases, the LUMOs are situated above the conduction band of TiO$_2$, whereas all the HOMOs are below the I$^-$/I$_3^-$ pair. The lowest HOMOs were found for the AzoTPPBr$_3$ isomers, followed by the AzoTPP and AzoTPP(TMS)$_3$ molecules, respectively. The AzoTPPBr$_3$ isomers exhibit the lowest LUMO values (therefore, they are closer to the CB of TiO$_2$), followed by *trans*-AzoTPP(TMS)$_3$, *cis*- and *trans*-AzoTPP, and *cis*-AzoTPP(TMS)$_3$, respectively (Figure 4). Furthermore, the results in Figure 4 indicate that the

HOMO−LUMO gaps vary from 2.57 eV (*trans*-AzoTPP-(TMS)$_3$) to 2.66 eV (*cis*-AzoTPP(TMS)$_3$). Both *trans*- and *cis*-AzoTPP isomers, as well as *cis*-AzoTPPBr$_3$, show a gap of 2.65 eV. The calculated gap for *trans*-AzoTPPBr$_3$ resulted to be 2.61 eV. All these values are higher by at least 0.28 eV with respect to the ZnTPP-C porphyrin. This means that the azo molecules that we considered here are not as good as the ZnTPP-C porphyrin that was reported before. However, the HOMO−LUMO gaps are close to the desirable values for different applications in solar cells. Therefore, AzoTPP and their derivatives could be considered for further development of novel DSSC. Moreover, if the azo compound attached to the conductor is still able to undergo a trans−cis photoisomerization, there could be an additional use as a molecular switch within the solar cell. According to our results, the use of TMS will cause the energy of the HOMO and the LUMO to increase marginally (with respect to AzoTPP, especially in the case of *cis*-AzoTPP(TMS)$_3$). This could improve the performance of the cell because the HOMO would be closer to the electrolyte redox potential whereas the LUMO would better approximate the CB of TiO$_2$.

The experimental UV−vis spectra of *trans*-AzoTPP and the cis isomer that is formed after UV irradiation were reported before[21] and are included in Figure 5 for comparison. Theoretical spectra are also reported.

The *trans*-AzoTPP spectrum shows five distinct bands, one of them of high intensity at 420 nm, and four low-intensity bands at 516, 562, 588, and 688 nm. For *cis*-AzoTPP, the intensity of the absorption band at 420 nm shows a decrement with respect to that of the trans isomer. An additional band of medium intensity appears at 448 nm, three low-intensity bands remain unchanged, and the band at 688 nm increases slightly. The emergence of the band at 448 nm and the decrease in intensity of the band at 420 nm reveal that the trans−cis isomerization of the synthesized azo compound takes place.[73] The low-intensity bands at $\lambda > 500$ nm are related to the porphyrin because they follow the same structure of the so-called Q-region. In general, the UV−vis spectra of porphyrins show also an excitation at about 400 nm (Soret band). Due to the change in intensity of the excitation at 420 nm, it is expected that this excitation arises from transitions with contributions from the azo group as well as contributions from the porphyrin (i.e., a charge transfer between the porphyrin and the azo group).

The results of the TDDFT calculations for the low intensity bands (Q-region) and high-intensity bands of the *trans*- and *cis*-AzoTPP species are presented in Table 1. This table reports the composition of the selected excitations in terms of the one-electron orbital transitions that make up each excitation. Only those contributions higher than 15% are included.

For comparison, Table 2 contains both the theoretical and the experimental absorption wavelengths of the Soret and Q-bands for TPP and *trans*-AzoTPP. The theoretical results of TPP match well with those from previous reports[73−75] and the calculated absorption wavelengths are in good agreement (error around 4%) with the experimental values. The origin of these excitations, all involve the HOMO−1 (H−1), HOMO (H), LUMO (L), and LUMO+1 (L+1), following the Gouterman four orbital model discussed elsewhere.[76−78] The results for *trans*-AzoTPP show that the absorption wavelengths of the Q-bands are sufficiently well reproduced (error about 13%), whereas the calculation of the Soret band provides better
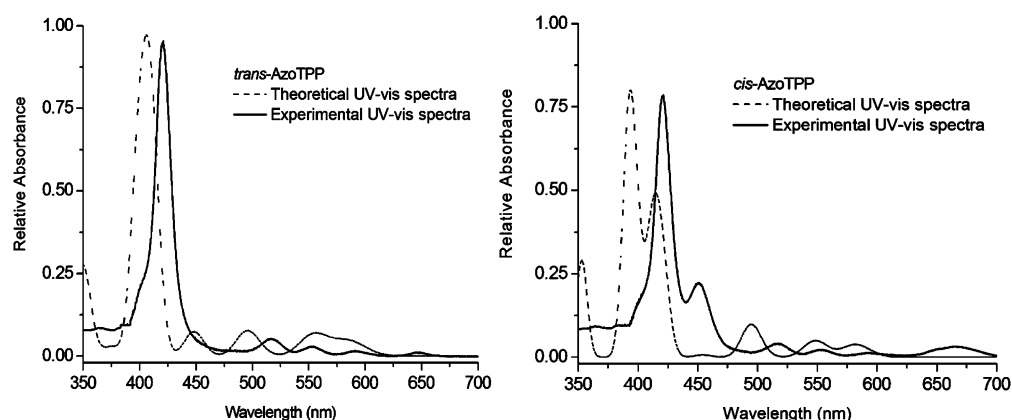
Figure 5. Experimental and theoretical UV−vis spectra of the *trans*-AzoTPP and the cis isomer formed after UV irradiation. The relative intensity of the theoretical spectra is taken with respect to the maximum of the *trans*-AzoTPP spectrum. The theoretical UV−vis spectra were simulated with Gaussview 5.0 using a peak half-width at half-maximum of 400 cm^{-1} and the type of broadening is Lorentzian.

Table 1. Calculated Low-Intensity Q-Bands and High Intensity Soret-Band Wavelengths (nm) and Their Oscillator Strengths (f) for TPP and *trans*- and *cis*-AzoTPP[a]

	λ (nm)	f	major orbital contributions to the transition[b]
			Q-Bands
TPP	579	0.0437	H → L (68%), H−1 → L+1 (31%)
	543	0.0663	H → L+1 (66%), H−1 → L (33%)
trans-AzoTPP	585	0.0709	H → L+1 (35%), H → L (31%), H−1 → L (16%)
	553	0.1338	H → L (43%), H → L+1 (27%), H−1 → L (15%)
	496	0.1419	H → L+2 (77%)
	450	0.0762	H−1 → L+2 (53%), H−1 → L (40%)
cis-AzoTPP	583	0.0755	H → L (39%), H → L+1 (30%)
	548	0.0987	H → L+1 (36%), H → L (33%), H−1 → L (18%)
	495	0.1961	H−2 → L+2 (47%), H → L+2 (28%)
	454	0.0139	H → L+2 (62%), H−2 → L+2 (20%)
			Soret Bands
TPP	405	1.3955	H−1 → L+1 (64%), H → L (28%)
	397	1.7377	H−1 → L (65%), H → L+1 (34%)
trans-AzoTPP	397	1.6079	H−1 → L+1 (34%), H−2 → L (20%)
	384	1.1097	H−1 → L+2 (26%), H−2 → L (16%), H−1 → L (16%)
cis-AzoTPP	420	0.5376	H−1 → L (39%), H−1 → L+2 (39%)
	412	0.6467	H−2 → L (41%), H−1 → L+1 (24%), H−2 → L+2 (16%)
	397	0.662	H−1 → L+2 (23%), H−2 → L (20%), H−1 → L+1 (15%)
	392	1.1425	H−1 → L+1 (20%), H−1 → L (16%) H−2 → LUMO (13%), H−1 → L+2 (13%)

[a]The orbital excitations that contribute more than 15% to the electronic transition are listed. [b]HOMO = H, LUMO = L.

results (error about 7%). In this case, additional contributions from the HOMO−2 and LUMO+2 orbitals are also computed.
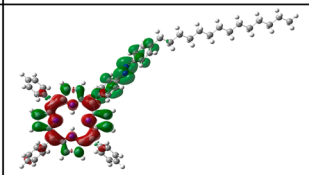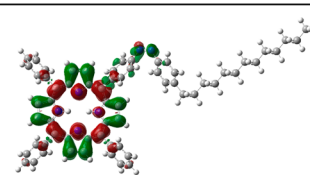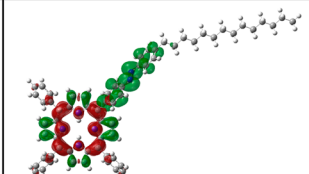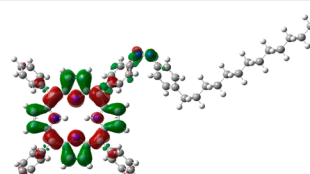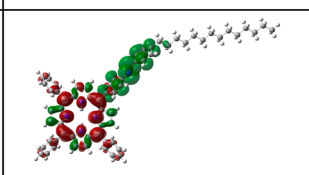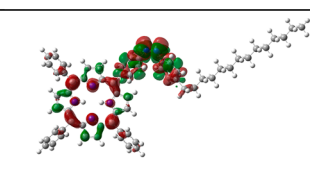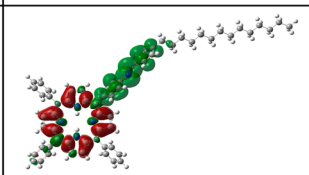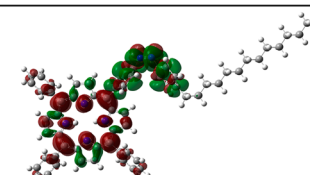
It was already discussed that the Q regions of the *trans*- and *cis*-AzoTPP species present the same structure. However, it is worthwhile to point out that according to our TDDFT calculations, the origin of the excitations that make up those bands seems to be of a different nature. Table 3 shows the electron density difference map (EDDM) for the excitations calculated in the Q region for the trans and cis isomers of AzoTPP. The EDDM shows the changes in electron density for a given excitation, where the electron density loss in the excitation is represented in red, and the green color indicates the electron density gain. As can be seen, the main differences between the EDDMs of the trans and cis isomers are due to the nature of the LUMO orbitals. Table 4 shows the HOMO, HOMO−1, HOMO−2, LUMO, LUMO+1, and LUMO+2 of the *trans*- and *cis*-AzoTPP isomers.

The HOMO, HOMO−1, and LUMO+1 orbitals are similar between the trans and cis isomers, but there is a remarkable difference in the LUMOs. The orientation of the phenyl group that is bonded to the porphyrin ring in *trans*-AzoTPP allows π interactions in the LUMO between the porphyrin, the phenyl, and the azo-phenyl groups. In contrast, the phenyl group in the LUMO of *cis*-AzoTPP does not show the same type of π interactions (Table 4). Thus, despite the similarities in the Q regions of both *trans*- and *cis*-AzoTPP spectra (Figure 5), the electron density loss-gain of each transition appears to be somewhat different (Table 3). In the case of the trans isomer, a charge transfer from the porphyrin to the azobenzene unit is clear. On the other hand, the change in electron density for the cis isomer takes place only within the porphyrin ring for the excitations calculated at 583 and 548 nm. Furthermore, the excitations at 495 and 454 nm take place mainly on the azobenzene units (Table 3). This occurs because the HOMO−2 and LUMO+2 are located only on the azobenzenes (Table

Table 2. Theoretical and Experimental Values of the Soret and Q-Bands for TPP and *trans*-AzoTPP

	TPP					*trans*-AzoTPP				
λ (nm)	Soret band	Q bands				Soret band	Q bands			
experimental	417	514	538	585	620	420	516	562	588	668
theoretical	405	543		579		397	450	496	553	585
	397					384				

Table 3. Electron Density Difference Map (EDDM) Calculated for the Electronic Excitations of *trans*- and *cis*-AzoTPP at the Q-Region[a]

trans-Azo TPP		*cis*-AzoTPP	
Theo. λ (nm)	EDDM	Theo. λ (nm)	EDDM
585		583	
553		548	
496		495	
450		454	

[a]Red: electron density loss in transition. Green: electron density gain in transition.

4), and the discussed excitations are made of transitions from HOMO−2 to LUMO+2.

As was mentioned above, the appearance of the additional band at 448 nm for the cis isomers is one of the main differences between the experimental spectra of the *trans*- and *cis*-AzoTPP species. This feature was theoretically reproduced as it can be seen in Figure 5.

Table 5 contains the EDDMs for the theoretical excitations at $\lambda \leq 420$ nm. For *cis*-AzoTPP, one excitation was calculated at 420 nm. We assigned this excitation as the one that gives rise to the "additional" cis band. The EDDM of this excitation shows a charge transfer from the porphyrin to the azobenzene moiety, mostly due to the HOMO−1 → LUMO+2 transition. The EDDMs for the most intense excitations (397 nm for *trans*-AzoTPP and 392 nm for *cis*-AzoTPP, respectively) are also shown in Table 5. The phenyl in *trans*-AzoTPP participates in the excitation due to the electronic transition to the LUMO. On the other hand, the predominance of the azo group in the *cis*-AzoTPP excitation could be traced back to the participation of the HOMO−2 and LUMO+2 orbitals in the transitions responsible of that excitation.

Concerning the derivatives where the porphyrin ring is substituted with TMS or Br groups, Table 6 shows the calculated low-intensity Q-band wavelengths and their respective oscillator strengths (f). It can be seen that there is no significant difference in the energy of the electronic absorption in this region, with respect to the AzoTPP molecule. However, it is worthwhile to point out that *trans*-AzoTPP-(TMS)$_3$ and *trans*-AzoTPPBr$_3$ generally absorb at slightly lower energy than *trans*-AzoTPP. According to Table 1 for the Q-

region, *trans*-AzoTPP absorbs in the range between 585 and 450 nm. For *trans*-AzoTPP(TMS)$_3$ the Q-bands are calculated to occur in the range between 588 and 449 nm, and from 585 to 431 nm in the case of *trans*-AzoTPPBr$_3$ (Table 6). The EDDMs for the excitations shown in Table 6 are included in the Supporting Information (Tables S3 and S4), where one can see that they follow the same pattern already discussed for the AzoTPP molecules.

Table 7 shows the calculated high-intensity Soret-region wavelengths and their oscillator strengths for the AzoTPPB$_3$ (B = TMS or Br) derivatives. The excitations with the highest intensities are calculated to appear at a moderately longer wavelength when compared to *trans*-AzoTPP. These excitations are calculated at 397, 401, and 411 nm for *trans*-AzoTPP, *trans*-AzoTPP(TMS)$_3$, and *trans*-AzoTPPBr$_3$, respectively. Thus, it would be expected to measure a more noticeable red shift, with respect to AzoTPP, of the Soret band in the experimental spectrum of AzoTPPBr$_3$. The EDDMs for the excitations shown in Table 7 are included in the Supporting Information (Tables S5 and S6).

The appearance of the "cis band" is also theoretically found (the simulated spectra are included in the Supporting Information, Figure S1). This excitation is calculated around 420 nm for *cis*-AzoTPP and *cis*-AzoTPP(TMS)$_3$. When Br is the substituent, the excitation appears at higher energy (402 nm).

If any of these porphyrins were used to build a solar cell, it might be useful that the cis band occurs closer to the most intense band. In this way, the absorption due to the n−π* band of the cis isomer could contribute to the operation of the solar

Table 4. HOMO, LUMO, HOMO−1, HOMO−2, LUMO+1, and LUMO+2 of the *cis*- and *trans*-AzoTPP Isomers

trans-AzoTPP		*cis*-AzoTPP	
L+2		L+2	
L+1		L+1	
LUMO		LUMO	
HOMO		HOMO	
H-1		H-1	
H-2		H-2	

Table 5. Electron Density Difference Map (EDDM) Calculated for the Excitations at $\lambda \leq 420$ nm for *trans*- and *cis*-AzoTPP[a]

trans-AzoTPP		*cis*-AzoTPP	
λ (nm)	EDDM	λ (nm)	EDDM
		420	'cis' band
397		392	

[a]Red: electron density loss in transition. Green: electron density gain in transition.

Table 6. Calculated Low-Intensity Q-Band Wavelengths (nm) and Their Oscillator Strengths (f) for the Derived Compounds *trans*-AzoTPP(TMS)$_3$, *trans*-AzoTPPBr$_3$, and Their Cis Isomers[a]

	λ (nm)	f	major orbital contributions to the transition[b]
trans-AzoTPP(TMS)$_3$	588	0.131	H → L (39%), H → L+1 (32%)
	557	0.2047	H → L (39%), H → L+1 (34%), H−1 → L (16%)
	498	0.1957	H → L+2 (77%), H−1 → L+1 (14%)
	449	0.2412	H−1 → L (48%), H−1 → L+2 (42%)
cis-AzoTPP(TMS)$_3$	584	0.0852	H → L (37%), H → L+1 (32%), H−1 → L+1 (15%)
	550	0.1161	H → L+1 (35%), H → L (34%), H−1 → L (17%)
	495	0.1968	H−2 → L+2 (47%), H → L+2 (29%)
trans-AzoTPPBr$_3$	585	0.0584	H → L+1 (46%), H−1 → L (22%), H → L (21%)
	551	0.1317	H → L (50%), H−1 → L+1 (20%)
	475	0.2445	H → L+2 (83%)
	431	0.1685	H−1 → L+2 (59%), H−1 → L (33%)
cis-AzoTPPBr$_3$	583	0.0464	H → L+1 (60%), H−1 → L (30%)
	548	0.0738	H → L (61%), H−1 → L+1 (28%)
	495	0.1375	H−2 → L+2 (59%)
	424	0.1725	H−2 → L (30%), H−2 → L+2 (26%), H−2 → L+1 (19%)

[a]The orbital excitations than contribute more than 15% to the electronic transition are listed. [b]HOMO = H, LUMO = L.

Table 7. Calculated Wavelengths (nm) (Soret Band, $\lambda \leq 420$ nm) and Oscillator Strengths (f) for *trans*-AzoTPP(TMS)$_3$, *trans*-AzoTPPBr$_3$, and Their Cis Isomers[a]

	λ (nm)	f	major orbital contributions to the transition[b]
trans-AzoTPP(TMS)$_3$	411	2.1049	H−1 → L+1 (44%), H−2 → L (18%), H → L+2 (15%)
	401	1.6065	H−1 → L+2 (44%), H−1 → L (20%), H → L+1 (21%)
cis-AzoTPP(TMS)$_3$	421	0.6581	H−1 → L (41%), H−1 → L+2 (36%)
	412	0.7531	H−2 → L (37%), H−1 → L+1 (27%)
	406	0.0963	H−2 → L+1 (72%), H−1 → L+2 (22%)
	399	0.6621	H−1 → L+2 (25%), H−2→L (21%)
	394	1.1583	H−1 → L+1 (21%), H−2 → L (17%)
trans-AzoTPPBr$_3$	401	1.5482	H−2 → L (37%), H−1 → L+1 (28%)
	388	0.8	H−1 → L+2 (27%), H−1 → L (20%)
cis-AzoTPPBr$_3$	402	0.4848	H−1 → L+2 (40%), H−1 → L (34%)
	389	0.5502	H−1 → L+2 (38%), H−1 → L+1 (14%)
	380	1.1316	H−1 → L+1 (38%), H−1 → L+2 (19%), H → L (20%)

[a]The orbital excitations than contribute more than 15% to the electronic transition are listed. [b]HOMO = H, LUMO = L.

compounds would act as electron acceptors with respect to $^\bullet O_2^-$. TiO$_2$ appears to be a better electron acceptor than these azo compounds. In all cases, the trans species are slightly better electron acceptors than their respective cis isomers.

AzoTPP and the derivatives reported here are promising materials for the construction of a novel dye-sensitized cell because the HOMO−LUMO gap is around 2 eV. Although the electronic absorption at this energy has a very low intensity (Q bands), the energy of the high intensity absorption bands fulfill the requirements needed for the operation of a solar cell prepared with TiO$_2$ and the I$^-$/I$_3^-$ pair.

The azo-dyes studied in this work exhibit strongly mixed configurations. All the electronic transitions follow Gouterman's four orbital model, as well as additional transitions involving other orbitals such as HOMO−2 and LUMO+2. Though the spectra of the trans and cis species are alike, the origin of the excitations is different. In the case of the trans isomers, the LUMO allows a charge transfer from the porphyrin ring to the azobenzene units. On the other hand, the cis configuration does not favor π interactions between the phenyl groups bonded to the azo bond and the porphyrin group.

The bands of all the azo compounds are estimated to occur at very similar energies. However, the n−π* band for the *cis*-AzoTPPBr$_3$ species appear closer to the most intense band, which makes AzoTPPBr$_3$ a more promising material for further development of a DSSC. Preparation of AzoTPPBr$_3$ and further experiments are needed to verify these theoretical predictions.

■ ASSOCIATED CONTENT

Ⓢ Supporting Information

Relative energy of the trans and cis isomers and main geometrical parameters of the compounds under study with their Cartesian coordinates; dihedral angles structures; theoretical energy difference; EDDMs for the calculated excitations of AzoTPPBr$_3$ and AzoTPP(TMS)$_3$ with the corresponding theoretical UV−vis spectra. This information is available free of charge via the Internet at http://pubs.acs.org

■ AUTHOR INFORMATION

Corresponding Author
*A. Martínez: e-mail, martina@unam.mx; tel, (52 55) 5622-4596.

Author Contributions
[†]These authors contributed equally to this work.

Notes
The authors declare no competing financial interest.

■ ACKNOWLEDGMENTS

■ REFERENCES

(1) Suijkerbuijk, B. M. J. M.; Gebbink, R. J. M. K. Merging Porphyrins with Organometallics: Synthesis and Applications. *Angew. Chem., Int. Ed.* **2008**, 47, 7396−7421.
(2) Senge, M. O.; Fazekas, M.; Notaras, E. G. A.; Blau, W. J.; Zawadzka, M.; Locos, O. B.; Mhuircheartaigh, E. M. N. Nonlinear Optical Properties of Porphyrins. *Adv. Mater.* **2007**, 19, 2737−2774.

cell, thereby counteracting the effect due to the intensity decrease of the main band after the photoisomerization process.

■ FINAL REMARKS

In general, the trans and cis isomers of the recently prepared AzoTPP, as well as some possible derivatives such as AzoTPP(TMS)$_3$ and AzoTPPBr$_3$ are not expected to undergo electron transfer reactions with reactive oxygen species such as $^\bullet$OH and $^\bullet$OOH. However, it is possible that these azo

(3) Pawlicki, M.; Collins, H. A.; Denning, R. G.; Anderson, H. L. Two-Photon Absorption and the Design of Two-Photon Dyes. *Angew. Chem., Int. Ed.* **2009**, *48*, 3244−3266.

(4) Anderson, H. L. Building Molecular Wires from the Colours of Life: Conjugated Porphyrin Oligomers. *Chem. Commun.* **1999**, 2323−2330.

(5) Jiang, L.; Li, Y. The Progress on Design and Synthesis of Photoactive Porphyrins-Based Dyads, Triads and Polymers. *J. Porphyrins Phthalocyanines* **2007**, *11*, 299−312.

(6) Petit, L.; Quartarolo, A.; Adamo, C.; Russo, N. Spectroscopic Properties of Porphyrin-Like Photosensitizers: Insights from Theory. *J. Phys. Chem. B* **2006**, *110*, 2398−2404.

(7) Wasielewski, M. R. Photoinduced Electron Transfer in Supramolecular Systems of Artificial Photosynthesis. *Chem. Rev.* **1992**, *92*, 435−461.

(8) Zaragoza-Galán, G.; Fowler, M.; Duhamel, J.; Rein, R.; Solladié, N.; Rivera, E. Synthesis and Characterization of Novel Pyrene Dendronized Porphyrins Exhibiting Efficient Fluorescence Resonance Energy Transfer: Optical and Photophysical Properties. *Langmuir* **2012**, *28*, 11195−11205.

(9) Ambroise, A.; Wagner, R. W.; Rao, P. D.; Riggs, J. A.; Hascoat, P.; Diers, J. R.; Seth, J.; Lammi, R. K.; Bocian, D. F.; Holten, D. Design and Synthesis of Porphyrin-Based Optoelectronic Gates. *Chem. Mater.* **2001**, *13*, 1023−1034.

(10) Liddell, P. A.; Kodis, G.; Moore, A. L.; Moore, T. A.; Gust, D. Photonic Switching of Photoinduced Electron Transfer in a Dithienylethene-Porphyrin-Fullerene Triad Molecule. *J. Am. Chem. Soc.* **2002**, *124*, 7668−7669.

(11) Aguilar-Ortiz, E.; Zaragoza-Galán, G.; Rein, R.; Solladié, N.; Aguilar-Martinez, M.; Macías-Ruvalcaba, N.; Rivera, E. Preparation and Characterization of Novel Polythiophenes Bearing Oligo(Ethylene Glycol) Spacers and Porphyrin Units: Optical and Electrochemical Properties. *Synth. Met.* **2012**, *162*, 1000−1009.

(12) Aziat, F.; Rein, R.; Peón, J.; Rivera, E.; Solladié, N. Polypeptides with Pendant Porphyrins of Defined Sequence of Chromophores: Towards Artificial Photosynthetic Systems. *J. Porphyrins Phthalocyanines* **2008**, *12*, 1232−1241.

(13) Camps, X.; Dietel, E.; Hirsch, A.; Pyo, S.; Echegoyen, L.; Hackbarth, S.; Roder, B. Globular Dendrimers Involving a C60 Core and a Tetraphenylporphyrine Function. *Chem.—Eur. J.* **1999**, *5*, 2362−2373.

(14) Brettar, J.; Gisselbrecht, J.-P.; Gross, M.; Solladié, N. Tweezers Hosts for Intercalation of Lewis Base Guests: Tuning Physico-Chemical Properties of Cofacial Porphyrin Dimers. *Chem. Commun.* **2001**, 733−734.

(15) Flamigni, L.; Talarico, A. M.; Ventura, B.; Rein, R.; Solladié, N. A Versatile Bis-Porphyrin Tweezer Host for the Assembly of Noncovalent Photoactive Architectures: A Photophysical Characterization of the Tweezers and Their Association with Porphyrins and Other Guests. *Chem.—Eur. J.* **2006**, *12*, 701−712.

(16) Knör, G. Intramolecular Charge Transfer Excitation of Meso-Tetrakis (1-Pyrenyl) Porphyrinato Gold (III) Acetate. Photosensitized Oxidation of Guanine. *Inorg. Chem. Commun.* **2001**, *4*, 160−163.

(17) Sheng, N.; Sun, J.; Bian, Y.; Jiang, J.; Xu, D. Synthesis and Third-Order Nonlinear Optical Properties of Novel Ethynyl-Linked Heteropentamer Composed of Four Porphyrins and One Pyrene. *J. Porphyrins Phthalocyanines* **2009**, *13*, 275−282.

(18) Zhu, M.; Lu, Y.; Du, Y.; Li, J.; Wang, X.; Yang, P. Photocatalytic Hydrogen Evolution Without an Electron Mediator Using a Porphyrin−Pyrene Conjugate Functionalized Pt Nanocomposite as a Photocatalyst. *Int. J. Hydrogen Energy* **2011**, *36*, 4298−4304.

(19) Bell, T. D. M.; Bhosale, S. V.; Ghiggino, K. P.; Langford, S. J.; Woodward, C. P. Synthesis and Photophysical Properties of a Conformationally Flexible Mixed Porphyrin Star-Pentamer. *Aust. J. Chem.* **2009**, *62*, 692−699.

(20) Balanay, M. P.; Kim, D. H. DFT/TD-DFT Molecular Design of Porphyrin Analogues for Use in Dye-sensitized Solar Cells. *Phys. Chem. Chem. Phys.* **2008**, *10*, 5121−5127.

(21) Caicedo, C.; Zaragoza-Galán, G.; Crusats, J.; El-Hachemi, Z.; Martínez, A.; Rivera, E. Design of Novel Luminescent Porphyrins Bearing Donor-Acceptor Groups. *J. Porphyrins Phthalocyanines* **2013**, DOI: 10.1142/S1088424613501083.

(22) Rau, H. In *Photochemistry and Photophysics*; Rabek, J. K., Ed.; CRC Press: Boca Raton, FL, 1990; Vol. 2, p 119.

(23) Natansohn, A.; Rochon, P. Photoinduced Motions in Azo-Containing Polymers. *Chem. Rev.* **2002**, *102*, 4139−4175.

(24) Loudwig, S.; Bayley, H. Photoisomerization of an Individual Azobenzene Molecule in Water: an On-Off Switch Triggered By Light at a Fixed Wavelength. *J. Am. Chem. Soc.* **2006**, *128*, 12404−12405.

(25) Bossi, M. L.; Murgida, D. H.; Aramendía, P. F. Photo-isomerization of Azobenzenes and Spirocompounds in Nematic and in Twisted Nematic Liquid Crystals. *J. Phys. Chem. B* **2006**, *110*, 13804−13811.

(26) Yagai, S.; Iwashima, T.; Kishikawa, K.; Nakahara, S.; Karatsu, T.; Kitamura, A. Photoresponsive Self-Assembly and Self-Organization of Hydrogen-Bonded Supramolecular Tapes. *Chem.—Eur. J.* **2006**, *12*, 3984−3994.

(27) Yamamoto, T.; Umemura, Y.; Sato, O.; Einaga, Y. Photo-magnetic Langmuir-Blodgett Films Consisting Azobenzene and Prussian Blue: Correlation Between the Film Structure and the Photomagnetic Efficiency. *Sci. Technol. Adv. Mater.* **2006**, *7*, 134−138.

(28) Takamatsu, D.; Yamakoshi, Y.; Fukui, K. Photoswitching Behavior of Nobel Single Molecular Tip of Noncontact Atomic Force Microscopy Designed for Chemical Identification. *J. Phys. Chem. B* **2006**, *110*, 1968−1970.

(29) Harbron, E. J.; Vicente, D. A.; Hadley, D. H.; Imm, M. R. Phototriggered Fluorescence Color Changes in Azobenzene-Functionalized Conjugated Polymers. *J. Phys. Chem. A* **2005**, *109*, 10846−10853.

(30) Rivera, E.; Carreon-Castro, M. P.; Rodríguez, L.; Cedillo, G.; Fomine, S.; Morales-Saavedra, O. G. Amphiphilic Azo-dyes (RED-PEGM). Part 2: Charge Transfer Complexes, Preparation of Langmuir-Blodgett Films and Optical. *Dyes Pigments* **2007**, *74*, 396−403.

(31) Rivera, E.; Carreón-Castro, M. P.; Buendía, I.; Cedillo, G. Optical Properties and Aggregation of Novel Azo-Dyes Bearing an End-Capped Oligo (Ethylene Glycol) Side Chain in Solution, Solid State and Langmuir-Blodgett Films. *Dyes Pigments* **2006**, *68*, 217−226.

(32) Rivera, E.; Belletête, M.; Natansohn, A.; Durocher, G. Synthesis, Characterization and Optical Properties of a Novel Azo-dye Bearing an Oligo(ethylene glycol) Methyl Ether Side Chain in Solution and in the Solid State. *Can. J. Chem.* **2003**, *81*, 1076−1082.

(33) Caicedo, C.; Rivera, E.; Valdez-Hernandez, Y.; Carreón-Castro, M. P. Synthesis and Characterization of Novel Liquid-crystalline Azo-dyes Bearing Two Amino-nitro Substituted Azobenzenes and a Well-defined Oligo(ethylene glycol) Spacer. *Mater. Chem. Phys.* **2011**, *130*, 471−480.

(34) Illescas, J.; Ramirez-Fuentes, Y. S.; Ortiz, J.; Esquivel, J.; Rivera, E.; Alzari, V.; Nuvoli, D.; Scognamillo, S.; Mariani, A. Preparation and Optical Characterization of Two Photoactive Poly(bisphenol A ethoxy diacrylate) Copolymers Containing Designed Amino-nitro Substituted Azobenzene Units, Obtained Via Classical and Frontal Polymerization, Using Novel Ionic Liquids as Initiators. *J. Polym. Sci. A: Polym. Chem.* **2012**, *50*, 1906−1916.

(35) García, T.; Carreón-Castro, M. P.; Gelover-Santiago, A.; Ponce, P.; Romero, M.; Rivera, E. Synthesis and Characterization of Novel Amphiphilic Azo-polymers Bearing Well-defined Oligo(ethylene glycol) Spacers. *Des. Monomers Polym.* **2012**, *15*, 159−174.

(36) Dircio, J.; Gelover-Santiago, A.; Caicedo, C.; Carreón-Castro, M. P.; Valdez-Hernandez, Y.; Rivera, E. Synthesis and Characterization of Novel Polythiophenes Containing Azobenzene Units and Well-defined Oligo(ethylene glycol) Spacers: Thermal and Optical Properties and Preparation of Langmuir Films. *Des. Monomers Polym.* **2012**, *15*, 175−195.

(37) Tapia, F.; Reyna-Gonzalez, J. M.; Huerta, G.; Almeida, S.; Rivera, E. Synthesis and Characterization of Novel Polythiophenes

Bearing Oligo(ethylene glycol) Segments and Azobenzene Units. *Polym. Bull.* **2010**, *64*, 581−594.

(38) Rivera, E.; Carreón-Castro, M. P.; Huerta, G.; Becerril, C.; Rivera, L.; Salazar, R. Synthesis and Characterization of Novel Grafted Azo-polymers Bearing Oligo(ethylene glycol) Spacers. *Polymer* **2007**, *48*, 3420−3428.

(39) Ortiz-Palacios, J.; Rodríguez-Alba, E.; Zaragoza-Galán, G.; Rivera, E. Fréchet-type Dendrons Bearing Azobenzene Units and Flexible Oligo(ethylene glycol) Spacers: Synthesis, Characterization, Thermal and Optical Properties. *Des. Monomers Polym.* **2013**, *16*, 578−591.

(40) Ortiz-Palacios, J.; Rodríguez-Alba, E.; Avelar, M.; Martínez, A.; Carreón-Castro, M. P.; Rivera, E. Synthesis and Characterization of Novel Dendrons Bearing Azobenzene Units and Oligo(ethylene glycol) Segments: Thermal, Optical Properties, Langmuir Films and Liquid Crystalline Behaviour. *Molecules* **2013**, *18*, 1502−1527.

(41) Lehn, J.-M. Conjecture: Imines as Unidirectional Photodriven Molecular Motors-Motional and Constitutional Dynamic Devices. *Chem.—Eur. J.* **2006**, *12*, 5910−5915.

(42) Kottas, G. S.; Clarke, L. I.; Horinek, D.; Michl, J. Artificial Molecular Rotors. *Chem. Rev.* **2005**, *105*, 1281−1376.

(43) Kinbara, K.; Aida, T. Toward Intelligent Molecular Machines: Directed Motions of Biological and Artificial Molecules and Assemblies. *Chem. Rev.* **2005**, *105*, 1377−1400.

(44) Muraoka, T.; Kinbara, K.; Aida, T. Mechanical Twisting of a Guest by a Photoresponsive Host. *Nature* **2006**, *440*, 512−515.

(45) Gust, D.; Moore, T. A.; Moore, A. L. Molecular Switches Controlled by Light. *Chem. Commun.* **2006**, 1169−1178.

(46) Rodríguez-Redondo, J. L.; Sastre-Santos, A.; Fernández-Lázaro, F.; Soares, D.; Azzellini, G. C.; Elliott, B.; Echegoyen, L. Phthalocyanine-Modulated Isomerization Behaviour of an Azo-Based Photoswitch. *Chem. Commun.* **2006**, 1265−1267.

(47) Ikeda, T.; Lintuluoto, J. M.; Aratani, N.; Yoon, Z. S.; Kim, D.; Osuka, A. Synthesis of Doubly Strapped meso−meso-Linked Porphyrin Arrays and Triply Linked Conjugated Porphyrin Tapes. *Eur. J. Org. Chem.* **2006**, 3193−3204.

(48) Cho, H. S.; Jeong, D. H.; Cho, S.; Kim, D.; Matsuzaki, Y.; Tanaka, K.; Tsuda, A.; Osuka, A. Photophysical Properties of Porphyrin Tapes. *J. Am. Chem. Soc.* **2002**, *124*, 14642−14654.

(49) Chen, Z.; Zhong, C.; Zhang, Z.; Li, Z.; Niu, L.; Bin, Y.; Zhang, F. Photoresponsive J-Aggregation Behavior of a Novel Azobenzene−Phthalocyanine Dyad and its Third-Order Optical Nonlinearity. *J. Phys. Chem. B* **2008**, *112*, 7387−7394.

(50) Caicedo, C.; Martinez, A.; Rivera, E. Theoretical Study of Novel Porphyrins Bearing Electron Donor−Acceptor Groups. *Int. J. Quantum Chem.* **2013**, *113*, 1376−1383.

(51) Hohenberg, P.; Kohn, W. Inhomogeneous Electron Gas. *Phys. Rev.* **1964**, *136*, B864.

(52) Kohn, W.; Sham, L. Self-Consistent Equations Including Exchange and Correlation Effects. *Phys. Rev.* **1965**, *140*, A1133.

(53) Frisch, M. J.; Trucks, G. W.; Schlegel, H. B.; Scuseria, G. E.; Robb, M. A.; Cheeseman, J. R.; Scalmani, G.; Barone, V.; Mennucci, B.; Petersson, G. A.; et al. *Gaussian 09*, Revision A.08; Gaussian, Inc.: Wallingford, CT, 2009.

(54) Becke, A. D. Density-Functional Thermochemistry. III. The Role of Exact Exchange. *J. Chem. Phys.* **1993**, *98*, 5648−5652.

(55) Lee, C.; Yang, W.; Parr, R. G. Development of the Colle-Salvetti Correlation-Energy Formula into a Functional of the Electron Density. *Phys. Rev. B* **1988**, *37*, 785−789.

(56) Stephens, P. J.; Devlin, F. J.; Chabalowski, C. F.; Frisch, M. J. Ab Initio Calculation of Vibrational Absorption and Circular Dichroism Spectra Using Density Functional Force Fields. *J. Phys. Chem.* **1994**, *98*, 11623−11627.

(57) Petersson, G. A.; Bennett, A.; Tensfeldt, T. G.; Al-Laham, M. A.; Shirley, W. A.; Mantzaris, J. A Complete Basis Set Model Chemistry. I. The Total Energies of Closed−Shell Atoms and Hydrides of the First−Row Elements. *J. Chem. Phys.* **1988**, *89*, 2193−2218.

(58) Petersson, G. A.; Al-Laham, M. A. A Complete Basis Set Model Chemistry. II. Open−Shell Systems and the Total Energies of the First−Row Atoms. *J. Chem. Phys.* **1991**, *94*, 6081−6090.

(59) Cancès, M. T.; Mennucci, B.; Tomasi, J. A New Integral Equation Formalism for the Polarizable Continuum Model: Theoretical Background and Applications to Isotropic and Anisotropic Dielectrics. *J. Chem. Phys.* **1997**, *107*, 3032−3041.

(60) Mennucci, B.; Tomasi, J. Continuum Solvation Models: A New Approach to the Problem of Solute's Charge Distribution and Cavity Boundaries. *J. Chem. Phys.* **1997**, *106*, 5151−5158.

(61) Jacquemin, D.; Perpète, E. A.; Ciofini, I.; Adamo, C. On the TD-DFT UV/vis Spectra Accuracy: The Azoalkanes. *Theor. Chem. Acc.* **2008**, *120*, 405−410.

(62) O'Boyle, N. M.; Tenderholt, A. L.; Langner, K. M. cclib: A Library for Package-Independent Computational Chemistry Algorithms. *J. Comput. Chem.* **2008**, *29*, 839−845.

(63) Gázquez, J. L. Perspectives on the Density Functional Theory of Chemical Reactivity. *J. Mex. Chem. Soc.* **2008**, *52*, 3−10.

(64) Gázquez, J. L.; Cedillo, A.; Vela, A. Electrodonating and Electroaccepting Powers. *J. Phys. Chem. A* **2007**, *111*, 1966−1970.

(65) Martínez, A.; Rodríguez-Gironés, M. A.; Barbosa, A.; Costas, M. Donator Acceptor Map for Carotenoids, Melatonin and Vitamins. *J. Phys. Chem. A* **2008**, *112*, 9037−9042.

(66) *CRC Handbook of Chemistry and Physics*, 87th ed.; Lide, D. R., Ed.; CRC Press: Boca Raton, FL, 2006; Section 9.

(67) Wazzan, N. A.; Richardson, P. R.; Jones, A. C. *Cis-Trans* Isomerisation of Azobenzenes Studied By Laser-Coupled NMR Spectroscopy and DFT Calculations. *Photochem. Photobiol. Sci.* **2010**, *9*, 968−974.

(68) Brown, E. V.; Granneman, G. R. *Cis-trans* Isomerism in the Pyridyl Analogs of Azobenzene. Kinetic and Molecular Orbital Analysis. *J. Am. Chem. Soc.* **1975**, *97*, 621−627.

(69) Hagfeldt, A.; Boschloo, G.; Sun, L.; Kloo, L.; Pettersson, H. Dye-Sensitized Solar Cells. *Chem. Rev.* **2010**, *110*, 6595−6663.

(70) Chiodo, L.; Salazar, M.; Romero, A. H.; Laricchia, S.; Della Sala, F.; Rubio, A. Structure, Electronic, and Optical Properties of TiO_2 Atomic Clusters: An ab Initio Study. *J. Chem. Phys.* **2011**, *135*, 244704.

(71) Fuke, N.; Fukui, A.; Islam, A.; Komiya, R.; Yamanaka, R.; Harima, H.; Han, L. Influence of TiO_2/Electrode Interface on Electron Transport Properties in Back Contact Dye-Sensitized Solar Cells. *Sol. Energy Mater. Sol. Cells* **2009**, *93*, 720−724.

(72) Hardin, B. E.; Snaith, H. J.; McGehee, M. D. The Renaissance of Dye-Sensitized Solar Cells. *Nat. Photonics* **2012**, *6*, 162−169.

(73) Kumar, G. S.; Neckers, D. C. Photochemistry of Azobenzene-Containing Polymers. *Chem. Rev.* **1989**, *89*, 1915−1925.

(74) Nemykin, V. N.; Hadt, R. G. Interpretation of the UV-vis Spectra of the Meso(Ferrocenyl)-Containing Porphyrins Using a TDDFT Approach: Is Gouterman's Classic Four-Orbital Model Still in Play? *J. Phys. Chem. A* **2010**, *114*, 12062−12066.

(75) Valiev, R. R.; Cherepanov, V. N.; Ya, V. Artyukhov, Dage Sundholm. Computational Studies of Photophysical Properties of Porphin, Tetraphenylporphyrin and Tetrabenzoporphyrin. *Phys. Chem. Chem. Phys.* **2012**, *14*, 11508−11517.

(76) Gouterman, M. Spectra of Porphyrins. *J. Mol. Spectrosc.* **1961**, *6*, 138−163.

(77) Gouterman, M.; Wagniere, G. H.; Snyder, L. C. Spectra of Porphyrins: Part II. Four Orbital Model. *J. Mol. Spectrosc.* **1963**, *11*, 108−127.

(78) Gouterman, M. Study of the Effects of Substitution on the Absorption Spectra of Porphin. *J. Chem. Phys.* **1959**, *30*, 1139−1162.